Active Noise Control System for Headphone Applications

Sen M. Kuo, *Senior Member, IEEE*, Sohini Mitra, and Woon-Seng Gan, *Senior Member, IEEE*

Abstract—**This paper presents the design and implementation of an adaptive feedback active noise control (ANC) system for headphone applications. The ideal position of the error microphone in the ear-cup was studied and determined experimentally, and music signals were used for adaptive system identification of the secondary path. The designed ANC headphone was implemented using the TMS320C32 digital signal processor for real-time experiments. Performance has been evaluated and compared with a high-end commercial ANC headphone using the same set of primary noises including real-world engine noises. Experiment results show the proposed ANC headphone achieves higher noise cancellation, especially for low-frequency harmonics.**

Index Terms—**Active noise control (ANC), adaptive feedback ANC systems, ANC headphones, error sensor optimization, secondary path modeling.**

I. INTRODUCTION

WITH the growth of technology and industry, acoustic noise problems have become more and more acute. Noise levels in human settings have come under scrutiny for reasons including health concerns and improvement of the quality of life. Common acoustic noises originate from the industrial products such as engines, blowers, fans, and transformers. For low-frequency noises, passive methods such as earmuffs are either ineffective or tend to be very expensive or bulky. Thus, the active noise control (ANC) systems [1]–[4], which efficiently attenuate low-frequency noises, have become an effective technique for designing ANC headphones to protect workers in noisy environments. The advent of fast computational devices such as digital signal processors has made the implementation of digital ANC headphone possible.

ANC headphone cancels the primary noise by introducing a secondary "antinoise" of equal amplitude but opposite phase, thus attenuating undesired acoustic noises inside the ear-cups. In feedforward ANC headphones, a reference microphone is placed outside the ear-cup to pick up the primary noise. This reference signal $x(n)$ is then processed by the ANC system to generate the control signal $y(n)$ to drive a secondary loudspeaker inside the ear-cup for producing antinoise. The error microphone monitors the performance of the ANC system by measuring the residual noise $e(n)$, which will be minimized by the adaptive algorithm. In this paper, we develop the adaptive feedback ANC (AFANC) system which uses the internal model (the estimated secondary path) to synthesize the reference signal $x(n)$ instead

S. M. Kuo and S. Mitra are with the Center for Acoustics and Vibration, Department of Electrical Engineering, Northern Illinois University, DeKalb, IL 60115 USA (e-mail: kuo@ceet.niu.edu).

W.-S. Gan is with the School of Electrical and Electronics Engineering, Nanyang Technological University, Singapore 639798.
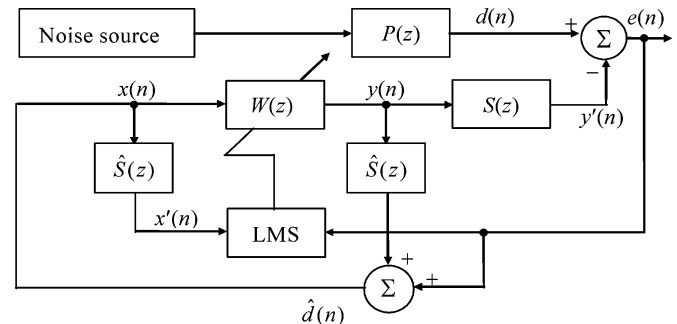
Fig. 1. Block diagram of adaptive feedback ANC system.

of using a reference microphone. Thus, the AFANC system uses only one error microphone per ear-cup, and results in a low-cost and compact ANC headphone design [5]. A comparative study of various AFANC systems using four different adaptive algorithms for headset applications is reported in [6].

In practical ANC systems, the secondary path $S(z)$ (see Fig. 1) includes the digital-to-analog converter (DAC), reconstruction filter, power amplifier, loudspeaker, acoustic path from loudspeaker to error microphone, error microphone, preamplifier, antialiasing filter, and analog-to-digital converter (ADC). The filtered-X least-mean-square (FXLMS) algorithm [7] places the secondary-path estimate in the reference signal path to the weight update of the algorithm. This secondary-path model is usually estimated by adaptive system identification using white noise as an excitation signal, which is annoying for headphone applications. The robustness of AFANC headset can be improved by adding an analog feedback loop to handle large secondary path flocculation [8]. In this paper, we study the feasibility of using music as an excitation signal for modeling secondary path and show it can achieve similar results as white noise and chirp signal.

The performance of ANC systems is determined by the magnitude response of the secondary path, which can be affected by the placement of the error microphone. In this paper, the optimum location of the error microphone is subject to the flat magnitude response of the secondary path, is found by experiments, and explained by the spectral filtering of pinna.

An ANC headphone was built for experiments by inserting an error microphone inside each ear-cup of a commercial audio headphone with a built-in loudspeaker. The AFANC algorithm was coded in assembly program and implemented on the Spectrum Signal Processing Inc. TMS320C32 processor board with 16-bit ADC and DAC on the 4 Channel Analog I/O Board for analog interface. Each of the four input channels and two output channels are provided with third-order Butterworth anti-aliasing filters. The cutoff frequency of these filters is set at 3.38 kHz with filter parameters given in the user's manual. The designed headphone was tested using sinusoidal noises generated by a

signal generator, and recorded engine noises for an engine running at 2200 and 3700 rpm. The emphasis of this paper is on the design and experiment of the AFANC headphone in real time, with the goal to achieve higher noise cancellation as compared to high-end commercial ANC headphones.

II. ADAPTIVE FEEDBACK ANC ALGORITHM

An AFANC system using the FXLMS algorithm is illustrated in Fig. 1, where the secondary signal is generated as [9]

$$y(n) = \mathbf{w}^T(n)\mathbf{x}(n) \tag{1}$$

where $\mathbf{w}(n)[w_0(n)\ w_1(n)\ \ldots\ w_{L-I}(n)]^T$ and are $\mathbf{x}(n) = [x(n)\,x(n-1)\ \ldots\ x(n-L+1)]^T$ the coefficient and signal vectors of $W(z)$, respectively, and L is the filter order. The adaptive filter minimizes the instantaneous squared error using the FXLMS algorithm

$$\mathbf{w}(n+1) = \mathbf{w}(n) + \mu \mathbf{x}'(n)e(n) \tag{2}$$

where $\mu > 0$ is the step size and

$$\mathbf{x}'(n) = \hat{s}(n) * \mathbf{x}(n) \tag{3}$$

is the filtered signal vector. In (3), $\hat{s}(n)$ is the impulse response of the secondary-path estimation filter $\hat{S}(z)$ and $*$ denotes linear convolution.

The primary noise $d(n)$ may not be available during the ANC operation. Therefore, a crucial step is to estimate the primary noise $d(n)$ and to use it as the reference signal $x(n)$ for the ANC filter $W(z)$ [1]. In the AFANC algorithm, the secondary-path estimate $\hat{S}(z)$ (see Fig. 1) is also used to synthesize the reference signal as

$$x(n) \equiv \hat{d}(n) = e(n) + \sum_{m=0}^{M-1} \hat{s}_m y(n-m-1) \tag{4}$$

where $\hat{s}_m, m = 0, 1, \ldots, M-1$ are the coefficients of the Mth order finite impulse response (FIR) filter $\hat{S}(z)$ used to estimate the secondary path $S(z)$. The required model $\hat{S}(z)$ can be estimated by adaptive system modeling techniques summarized in [2] using white noise. In this paper, we use music as an excitation signal for adaptive system identification.

For perfect cancellation, the error signal should become zero, which requires the adaptive filter to converge to the optimum transfer function expressed as

$$W^o(z) = \frac{P(z)}{S(z)}. \tag{5}$$

Therefore, the adaptive filter models the primary path $P(z)$ (see Fig. 1) and inversely models the secondary path $S(z)$. However, the behavior and performance of the ANC system is mainly determined by the secondary path $S(z)$, which is the target for optimization in this paper. Equation (5) shows that the ANC system is unstable if there is a frequency ω_0 such that $S(\omega_0) = 0$. Therefore, the FXLMS algorithm works properly for all frequencies when the magnitude response of the secondary path is flat. In this paper, we study the effects of the error microphone

Fig. 2. Experimental setup for designing and testing AFANC headphone.

location on the secondary-path magnitude response, and determine the ideal location inside the ear-cup that achieves flat magnitude response.

III. SECONDARY PATH OPTIMIZATION AND MODELING

Fig. 2 shows the experimental setup for designing and testing the AFANC headphone. An HP3563A Control Systems Analyzer is used to measure the performance (spectra) and estimate the transfer function of the secondary path. Instead of building a new headphone, we modify the commercial audio headphone Sennheiser HD 565 Ovation by adding an error microphone into each ear-cup. As shown in Fig. 2, this headphone is mounted on a KEMAR (Knowles electronics mannequin for acoustics research) mannequin, which has a $1/2''$ Falcon range microphone type 4189 installed inside the ear cavity of the KEMAR. An ONKYO stereo amplifier is used to amplify the signal being fed to the loudspeaker inside the headphone. The error signal is picked up by an omni-directional Realistic tie-pin microphone embedded inside the ear-pad of the headphone. The error microphone signal is pre-amplified by a Symetrix SX202 dual preamplifier.

A. Placement of Error Microphone

The spectral filtering of a sound source that is caused primarily by the outer ear (pinna) will affect the secondary-path transfer function $S(z)$. The asymmetrical, complex construction of the outer ears cause a unique set of delays, resonances, and diffractions that collectively translate into a unique transfer function for each microphone position [10]. Intensive experiments were conducted to find the optimum location for the design of the AFANC headphone. The sampling frequency chosen for the measurements is 8 kHz, and the frequency range of interest being between 0–3.38 kHz.

As illustrated in Fig. 3, the secondary path estimation is conducted for eight different error microphone locations on the median plane around the ear-pad of the headphone. The positions #6, #7, and #8 are clearly identified (with arrows) in Fig. 2. For each microphone position, the corresponding secondary-path transfer function is measured using the HP3563A
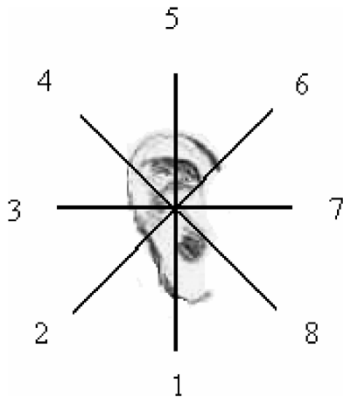
Fig. 3. Error microphone locations corresponding to the ear surface.

analyzer. There was a marked dissimilarity between the frequency responses obtained for locations one to four and those obtained for locations five to eight, which corresponds to the posterior and frontal parts of the external ear, respectively. This is because these two parts of the external ear differ significantly in the distribution of cartilaginous framework of elastic connective tissue. The cartilage and skin in the frontal portion of the external ear appear in the form of multiple folds which forms a kind of hollow with the external auditory meatus extending from the pinna to the ear drum. On the other hand, the posterior portion of the external ear consists of a folded rim of skin and cartilage around most of the portion of the outer ear. It was observed that for error microphone locations five to eight, there was a marked similarity in the frequency responses.

As expressed in (5), the optimum error microphone location for the ANC system was chosen based on the flatness of the magnitude response measured at that location. It was observed that the system showed the flattest frequency response with least number of dips and peaks at the microphone locations #8. Fig. 4 compares the magnitude response of the worst transfer function (position #2) with the best transfer function measured at position #8. Fig. 4 also shows the magnitude responses of positions #4 and #6 for reference. Since position #8 is near the external auditory meatus, the microphone could fit in more easily inside the hollow in that location.

Because the objective of ANC headphones is to reduce the noise that is heard by the ear, Fig. 5 shows that the magnitude response measured at location #8 matches with the microphone installed inside the ear cavity of the KEMAR. This figure proves that the error microphone at location #8 will result in the best noise reduction in the ear hearing position as well. Therefore, position #8 is chosen to be the optimal error microphone location for the design of the AFANC headphone.

B. Excitation Signals

The excitation signals used for adaptive system identification should ideally have a constant spectral density at all frequencies. The most commonly used training signals are white noise and chirp signals. However, it is desirable to use music since the training signal is heard for headphone applications. Music signals [11] are extremely variable in their complexity and may range from a near sine waveform of a single musical instrument

or voice, to the highly complex mixed sound of a symphony orchestra. Two very common characteristics were observed for most of the music pieces analyzed. Pieces of music, which were rich in frequency contents, had a smaller frequency range. Those pieces, which had a wider frequency range, had a lower frequency density. For the pieces from "O Fortuna from Carmina Burana," a number of consecutive frames were found to be rich in frequency contents, and it was almost flat in the frequency range from 0–4 kHz.

The effectiveness of the music piece as an excitation signal in adaptive system modeling was evaluated and compared with that of conventional training signals like white noise and chirp signal. Fig. 6 shows the magnitude responses of $S(z)$ and its estimate using music. As shown in the figure, the magnitude response is estimated using music signal and is closely matched to the system to be modeled.

IV. REAL-TIME EXPERIMENTS

A real-time experiment of the designed AFANC headphone was conducted in the Digital Signal Processing (DSP) lab at Northern Illinois University. The surrounding environment in the DSP lab (see Fig. 2) closely resembles real-life settings with sound reflections from various objects in the room. Primary noises used for real-time experiments are sinusoidal noises at different frequencies and engine noises at 2200 rpm and 3700 rpm. Performance of the ANC headphones was evaluated using the built-in microphone inside the ear canal of the KEMAR. Therefore, the measured noise cancellation would be very close to what would actually be perceived by the human ear in a real-life situation. The noise cancellation performance obtained was compared with that of a leading commercial headphone by mounting the commercial ANC headphone on the KEMAR under the identical testing parameters.

As shown in Fig. 2, the headphone is mounted on a KEMAR mannequin, which is placed on a chair. The engine noise is played from a Sony Digital Audio Tape (DAT) deck. For all the experiments conducted, the primary loudspeaker is placed facing the KEMAR, 27 cm in front and 24 cm below. With the error microphone placed at the optimum location #8 (see Fig. 2), noise cancellation tests have been conducted for different primary noises. The length of the filter $\hat{S}(z)$ for modeling of the secondary path is 65, and the step size is 0.05. The length of the adaptive filter $W(z)$ used for the noise cancellation is 110, and the step-size μ is 0.3.

For the first set of real-time experiments, sinusoidal noises in the range of 0–2 kHz with the step of 100 Hz were generated using an HP 33120A signal generator. Fig. 7 depicts the noise cancellation results obtained in real time for sinusoidal frequencies at intervals of 100 Hz. It is observed that even though the net noise cancellation (the difference between ANC OFF and ON) decreases with increase in frequency, it is considerably high (more than 50-dB attenuation) for frequencies all the way up to 2 kHz.

Real-time performance for the designed AFANC headphone was also tested for engine noises recorded at a fixed 2200 rpm and 3700 rpm. The engine noise was played through the Sony
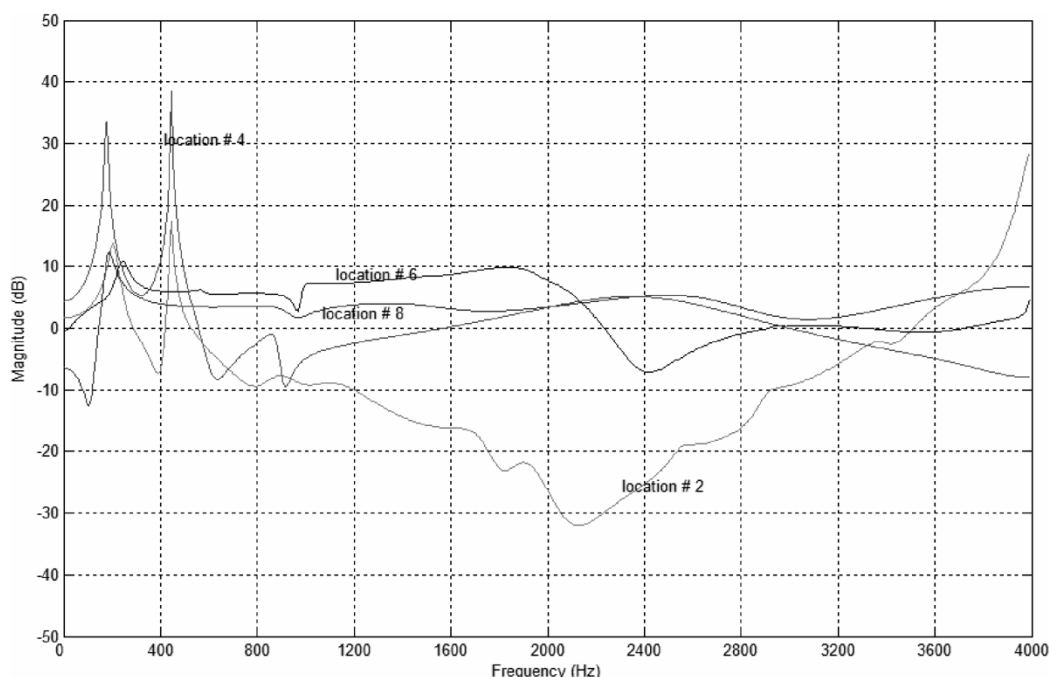
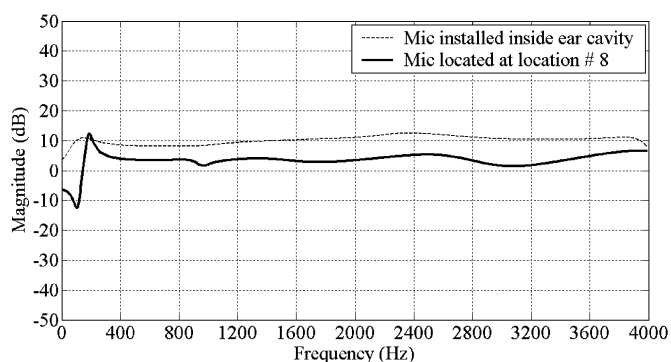Fig. 4.   Magnitude responses of $S(z)$ at different microphone locations.

Fig. 5.   Magnitude responses of $S'(z)$ at microphone location #8 and inside the ear cavity.
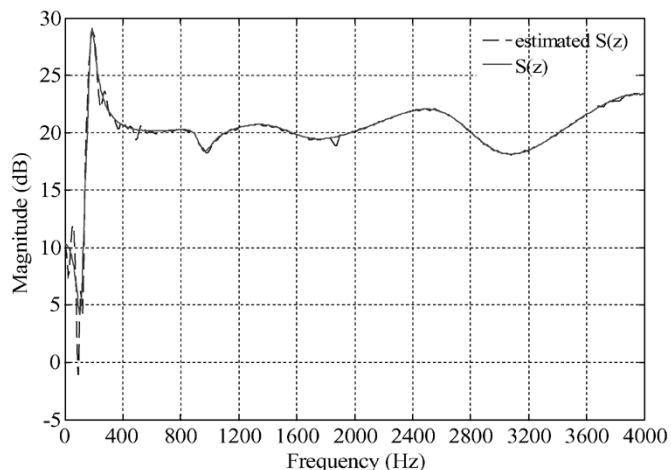

Fig. 6.   Magnitude responses of $S(z)$ and its estimate using music as excitation signals.
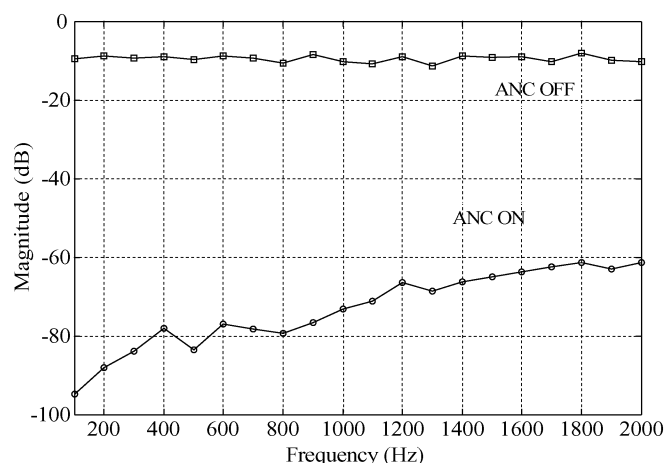

Fig. 7.   Noise cancellation levels for sinusoidal primary noise at different frequencies.

picts the residual noise obtained after cancellation. Note that both noises are measured from the built-in microphone inside the KEMAR's ear. Fig. 8 shows considerable noise cancellation for the first three harmonic components. The noise cancellation levels at 61, 122, and 183 Hz are 20.906, 18.387, and 16.293 dB, respectively.

The noise cancellation of the AFANC algorithm was repeated for the engine noise recorded at 2200 rpm, and its real-time performance is depicted in Fig. 9. The dotted line depicts the power spectrum of the engine noise, and the solid line depicts the residual noise obtained after cancellation. The noise cancellation levels for harmonic components at 76, 116, 156, and 196 Hz are 14.371, 25.627, 26.767, and 13.197 dB, respectively.

Finally, the performance of the AFANC headphone designed in this paper was compared to that of the leading commercial ANC headphone. In both cases, the noise cancellation was

DAT deck. The dotted line on Fig. 8 depicts the power spectrum of the engine noise at 3700 rpm, and the solid line de-
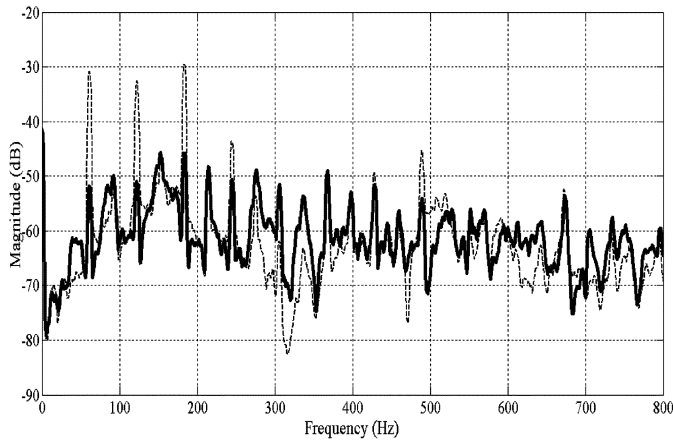
Fig. 8.   Power spectra for the original engine noise at 3700 rpm (dotted line) and the residual noise (solid line) after noise control.
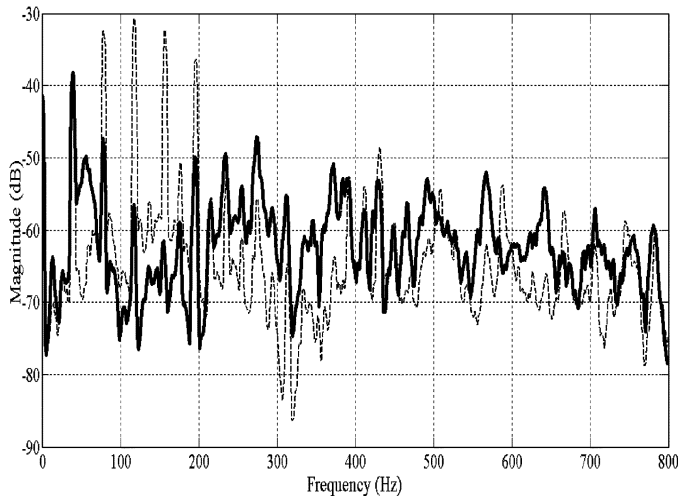

Fig. 9.   Power spectra for engine noise at 2200 rpm (dotted line) and the residual noise (solid line) after ANC.
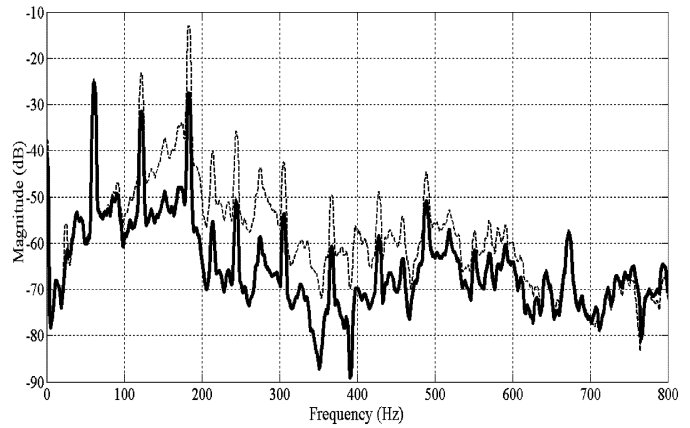

Fig. 10.   Power spectra for the original engine noise at 3700 rpm (dotted line) and the residual noise (solid line) for a Bose QuietComfort 2 ANC headphone.

Again, we achieve a marked improvement in noise cancellation in comparison to the leading commercial ANC headphone.

V. CONCLUSION

In this paper, an adaptive feedback ANC headphone has been designed using the FXLMS algorithm. Conventional excitation signals such as white noise and chirp signal have been replaced by music signals for modeling the secondary-path transfer function. The performance of the music piece as a training signal for adaptive system modeling was similar with that of white noise and chirp signal. The optimum error microphone location for the AFANC headphone has been studied and found experimentally. The designed AFANC headphone was implemented on the TMS320C32 using assembly program for real-time experiments. Higher noise cancellation has been achieved by comparing with that of the high-end commercial ANC headphone.

monitored by the built-in microphone inside the KEMAR's ear canal. As shown in Fig. 8, for engine noise at 3700 rpm, the noise cancellation levels for the designed Northern Illinois University (NIU) ANC headphone are 20.906, 18.387, and 16.293 dB for harmonics at 61, 122, and 183 Hz, respectively. This experiment is repeated by mounting the leading commercial ANC headphone on the KEMAR, and the spectral plot shown in Fig. 10 was obtained using the HP3563A analyzer. The noise cancellation levels using the commercial ANC headphone for those three harmonics are 0.685, 8.284, and 14.575 dB. Thus, the headphone designed in this paper has achieved a significant improvement in noise cancellation for all three harmonics, especially at low frequencies.

Similarly, this experiment was repeated for engine noise at 2200 rpm. As shown in Fig. 9, the noise cancellation levels obtained for the designed AFANC headphone are 14.371, 25.627, 26.767, and 13.197 dB for harmonics at 76, 116, 156, and 196 Hz, respectively. Under the identical testing environment, the corresponding noise cancellation levels obtained using the commercial ANC headphone are 0.919, 6.955, 12.25,and 13.409 dB.

REFERENCES

[1] S. M. Kuo and D. R. Morgan, "Active noise control: a tutorial review," *Proc. IEEE*, vol. 8, no. 6, pp. 943–973, Jun. 1999.

[2] ——, *Active Noise Control Systems: Algorithms and DSP Implementations*.   New York: Wiley, 1996.

[3] P. A. Nelson and S. J. Elliott, *Active Control of Sound*.   San Diego, CA: Academic, 1992.

[4] S. J. Elliott, *Signal Processing for Active Control*.   San Diego, CA: Academic, 2001.

[5] W. S. Gan and S. M. Kuo, "An integrated audio and active noise control headsets," *IEEE Trans. Consum. Electron.*, vol. 48, no. 2, pp. 242–247, May 2002.

[6] B. Siravara, M. Mansour, R. Cole, and N. Mogotra, "Comparative study of wideband single reference active noise cancellation algorithms on a fixed-point DSP," in *Proc. ICASSP*, 2003, pp. II-473–II-476.

[7] D. R. Morgan, "An analysis of multiple correlation cancellation loops with a filter in the auxiliary path," *IEEE Trans. Acoust. Speech, Signal Process.*, vol. ASSP-28, no. 4, pp. 454–467, Aug. 1980.

[8] Y. Song, Y. Gong, and S. M. Kuo, "A robust hybrid feedback active noise cancellation headset," *IEEE Trans. Speech Audio Process.*, vol. 13, no. 4, pp. 607–617, Jul. 2005.

[9] S. M. Kuo, X. Kong, and W. S. Gan, "Applications of adaptive feedback active noise control system," *IEEE Trans. Contr. Syst. Technol.*, vol. 11, no. 2, pp. 216–220, Mar. 2003.

[10] D. R. Begault, *3-D Sound for Virtual Reality and Multimedia*.   San Diego, CA: Academic, 1994.

[11] J. F. Alm and J. S. Walker, "Time frequency analysis of musical instruments," *Soc. Indust. Appl. Math.*, vol. 44, no. 3, pp. 457–476, 2002.